The D614G mutation of SARS-CoV-2 spike protein enhances viral infectivity and decreases neutralization sensitivity to individual convalescent sera

— Source link ↗

Jie Hu, Chang Long He, Qingzhu Gao, Gui Ji Zhang ...+8 more authors

Institutions: Laboratory of Molecular Biology

Published on: 20 Jun 2020 - bioRxiv (Cold Spring Harbor Laboratory)

Topics: Entry into host and Infectivity

Related papers:

- D614G mutation of SARS-CoV-2 spike protein enhances viral infectivity

- Tracking Changes in SARS-CoV-2 Spike: Evidence that D614G Increases Infectivity of the COVID-19 Virus.

- The D614G mutation in the SARS-CoV-2 spike protein reduces S1 shedding and increases infectivity

- A pneumonia outbreak associated with a new coronavirus of probable bat origin

- Structure, Function, and Antigenicity of the SARS-CoV-2 Spike Glycoprotein.

1   **D614G mutation of SARS-CoV-2 spike protein enhances viral infectivity**

2   ***Running Title：*** D614G mutant spike increases SARS-CoV-2 infectivity

3   Jie Hu[1, #], Chang-Long He[1, #], Qing-Zhu Gao[1, #], Gui-Ji Zhang[1 #], Xiao-Xia Cao[1],

4   Quan-Xin Long[1], Hai-Jun Deng[1], Lu-Yi Huang[1], Juan Chen[1], Kai Wang[1,*], Ni

5   Tang[1,*], Ai-Long Huang[1,*]

6

7   [1]Key Laboratory of Molecular Biology for Infectious Diseases (Ministry of

8   Education), Institute for Viral Hepatitis, Department of Infectious Diseases, The

9   Second Affiliated Hospital, Chongqing Medical University, Chongqing, 400010,

10   China

11   [#]These authors contributed equally to this work.

12

13   **Corresponding authors:*

14   Ai-Long Huang, Ni Tang, Kai Wang, Key Laboratory of Molecular Biology for

15   Infectious Diseases (Ministry of Education), Institute for Viral Hepatitis, Department

16   of Infectious Diseases, The Second Affiliated Hospital, Chongqing Medical

17   University, Chongqing, China. Phone: 86-23-68486780, Fax: 86-23-68486780, E-

18   mail: ahuang@cqmu.edu.cn (A.L.H.), nitang@cqmu.edu.cn (N.T.),

19   wangkai@cqmu.edu.cn (K.W.)

20

Abstract

Coronavirus disease 2019 (COVID-19) is caused by severe acute respiratory

syndrome coronavirus 2 (SARS-CoV-2). The spike (S) protein that mediates

SARS-CoV-2 entry into host cells is a major target for vaccines and therapeutics.

Thus, insights into its sequence variations are key to understanding the infection

and antigenicity of SARS-CoV-2. A dominant mutational variant at position 614 of

the S protein (aspartate to glycine, D614G mutation) was observed in the SARS-

CoV-2 genome sequence obtained from the Nextstrain database. Using a

pseudovirus-based assay, we identified that S-D614 and S-G614 protein

pseudotyped viruses share a common receptor, human angiotensin-converting

enzyme 2 (ACE2), which could be blocked by recombinant ACE2 with the fused Fc

region of human IgG1. However, S-D614 and S-G614 protein demonstrated

functional differences. First, S-G614 protein could be cleaved by serine protease

elastase-2 more efficiently. Second, S-G614 pseudovirus infected 293T-ACE2

cells significantly more efficiently than did the S-D614 pseudovirus, especially in

the presence of elastase-2. Third, an elastase inhibitor approved for clinical use

blocked elastase-enhanced S-G614 pseudovirus infection. Moreover, 93% (65/70)

convalescent sera from patients with COVID-19 could neutralize both S-D614 and

S-G614 pseudoviruses with comparable efficiencies, but about 7% (5/70)

convalescent sera showed reduced neutralizing activity against the S-G614

pseudovirus. These findings have important implications for SARS-CoV-2

transmission and immune interventions.

43   **Keywords:** antiviral therapeutics, coronavirus, COVID-19, D614G mutation,

44   infectivity, neutralizing antibodies, pseudovirus, SARS-CoV-2, spike protein

45

46   **Introduction**

47   Severe acute respiratory syndrome coronavirus 2 (SARS-CoV-2) is a novel

48   coronavirus reported in 2019 that caused the recent outbreak of coronavirus

49   disease 2019 (COVID-19)[1]. By July 4, 2020, the World Health Organization (WHO)

50   reported that 10.92 million people worldwide had been infected with SARS-CoV-2,

51   and that 523 000 individuals had died of COVID-19. This pandemic has had a

52   significant adverse impact on international, social, and economic activities.

53   Coronaviruses are enveloped, positive-stranded RNA viruses that contain the

54   largest known RNA genomes to date. The RNA genome of SARS-CoV-2 has been

55   rapidly sequenced to facilitate diagnostic testing, molecular epidemiologic source

56   tracking, and development of vaccines and therapeutic strategies[2]. The mutation

57   rate for RNA viruses is extremely high, which may contribute to their transmission

58   and virulence. The only significant variation in the SARS-CoV-2 spike (S) protein is

59   a non-synonymous D614G (aspartate (D) to glycine (G)) mutation[3]. Primary data

60   showed that S-G614 is a more pathogenic strain of SARS-CoV-2 with high

61   transmission efficiency[3]. However, whether the D614G mutation in the S protein

62   affects viral entry and infectivity in a cellular model is still unclear.

63

64   The S protein of coronavirus, the major determinant of host and tissue tropism, is a

3

65   major target for vaccines, neutralizing antibodies, and viral entry inhibitors[4,5].

66   Similar to SARS-CoV, the cellular receptor of SARS-CoV-2 is angiotensin-

67   converting enzyme 2 (ACE2); however, the SARS-CoV-2 S protein has a 10- to

68   20-fold higher affinity for ACE2 than the corresponding S protein of SARS-CoV[6,7].

69   Coronaviruses use two distinct pathways for cell entry: protease-mediated cell-

70   surface and endosomal pathways[8]. The S proteins of several coronaviruses are

71   cleaved by host proteases into S1 subunit for receptor binding and S2 subunit for

72   membrane fusion at the entry step of infection. Several cellular proteases including

73   furin, transmembrane protease serine 2 (TMPRSS2), and cathepsin (Cat) B/L are

74   critical for priming the SARS-CoV-2 S protein to enhance ACE2-mediated viral

75   entry[4]. Recently, Bhattacharyya et al. (2020) reported that a novel serine protease

76   (elastase-2) cleavage site was introduced into the S-G614 protein of SARS-CoV-

77   2[9]. However, it is unknown whether the S-G614 protein can be processed and

78   activated by elastase-2 in a cellular model. The S protein plays a key role in the

79   evolution of coronaviruses to evade the host immune system. It is still uncertain

80   whether the D614G mutation affects the antigenic properties of the S protein.

81   Meanwhile, whether elastase-2 inhibitors and convalescent serum samples of

82   COVID-19 can block the infection of the D614G variant of SARS-CoV-2 remains

83   unknown.

84

85   In this study, we analyzed the S gene sequences of SARS-CoV-2 submitted to the

86   Global Initiative on Sharing All Influenza Data (GISAID) database. We examined

4

87   the expression and cleavage of S-D614 and S-G614 protein in cell lines. Using a

88   luciferase (Luc)-expressing lentiviral pseudotype system, we established a

89   quantitative pseudovirus-based assay for the evaluation of SARS-CoV-2 cell entry

90   mediated by the viral S protein variants. We also compared the neutralizing

91   sensitivity of the S-D614 and S-G614 protein pseudoviruses to convalescent sera

92   from patients with COVID-19. Our study provides further insights into the

93   transmission and immune interventions of this newly emerged virus.

94

95   **Results**

96   **D614G mutation of SARS-CoV-2 S protein was globally distributed**

97   The S protein of SARS-CoV-2, which contains 1,273 amino acids, forms a trimeric

98   spike on the virion surface and plays an essential role in viral entry. We analyzed

99   the SARS-CoV-2 S protein amino acid sequence from viral genomic sequences in

100   the GISAID database. In line with prior reports, we found a globally distributed S

101   protein mutation, D614 to G614, which represented 64.6% of all the analyzed

102   sequences (Fig. 1 and Table 1). Among the top 10 most abundant non-

103   synonymous mutations observed in the S protein, the relative abundance of the

104   D614G mutant (the clade G) was the highest around the world, indicating that

105   G614 strain may be selectively advantageous. Since the S protein is critical to

106   coronavirus infection, we sought to explore the potential impact of the most

107   prevalent D614G mutation on the S protein structure, expression, and function.

108   Using the cryo-electron microscopy structure of S protein (PBD ID: 6ZGE)

109   determined by Wrobel et al.[10], we analyzed the potential effects of the D614G

110   mutation. As shown in Fig. 1b, residue D614 is located at the C-terminal region of

111   the S1 domain, which directly associates with S2. On the one hand, residue D614

112   forms a hydrogen bond with backbone of G593 and a salt bridge with K854, and

113   then is capped by the folded 833-855 motif of chain B (Fig. 1c). D614G mutation

114   would abolish these interactions. This change may destabilize the locked

115   conformation to promote receptor binding domain (RBD) opening and potentially

116   increase virus-receptor binding and membrane fusion activities. On the other hand,

117   we observed that D614 is remarkably close to the N-linked glycosylation site N616

118   (Fig 1c). Thus, the D614G mutation may enhance the fitness of SARS-CoV-2 by

119   increasing S protein stability and participating in glycosylation. Further studies are

120   required to determine the structure of S-G614 protein.

121

122   **D614G mutation enhanced the cleavage of S protein variant by proteases**

123   As the D614G mutation is proximal to the S1 cleavage domain, we predicted

124   potential cleavage sites of proteases in S protein variants using PROSPER[11], and

125   identified a novel serine protease (elastase-2) cleavage site at residues 615-616

126   on the S1-S2 junction of the S-G614 protein (Fig. 2a, Supplementary information,

127   Table S2). To evaluate the expression and cleavage of SARS-CoV-2 S protein in a

128   human cell line, the codon-optimized S protein-expressing plasmids (pS-D614 and

129   pS-G614) were transfected into HEK 293T cells. The immunoblot analysis of

130   whole cell lysates revealed that both S-D614 and S-G614 proteins showed two

131   major protein bands (unprocessed S and cleaved S1 subunit), when allowed to

132   react with the monoclonal antibody targeting the RBD on the SARS-CoV-2 S

133   protein (Fig. 2b). However, the pS-G614-transfected cells showed a stronger S1

134   signal than pS-D614-transfected cells, indicating that the D614G mutation altered

135   the cleavability of the S protein by cellular proteases. Moreover, the elastase

136   inhibitor sivelestat sodium significantly decreased the S1 signal of S-D614 protein

137   (Fig. 2b). These data indicate that the D614G mutation of SARS-CoV-2 S

138   facilitates its cleavage by host serine protease elastase-2. The coronavirus S

139   protein must be cleaved by host proteases to enable membrane fusion, which is

140   critical for viral entry. Next, we sought to explore the impact of D614G mutation on

141   viral entry.

142

143   **Evaluating viral entry efficacies between S-D614 and S-G614 pseudotyped**

144   **lentiviral particles**

145   Lentiviral vectors can be pseudotyped with various heterologous viral

146   glycoproteins that modulate cellular tropism and entry properties[12]. Due to the

147   highly pathogenic nature of SARS-CoV-2, infectious SARS-CoV-2 must be

148   handled in a biosafety level 3 (BSL-3) facility. We generated pseudotyped SARS-

149   CoV-2 based on the viral S protein using a lentiviral system, which introduced a

150   Luc (luciferase) reporter gene for quantification of SARS-CoV-2 S-mediated entry.

151   Thereafter, pNL4-3.Luc.R-E- was co-transfected with pS-D614 and pS-G614 to

152   package the SARS-CoV-2 S pseudotyped single-round Luc virus in HEK 293T

7

153   cells.

154   The titers of S-D614 and S-G614 protein pseudotyped viruses were determined by

155   reverse transcriptase quantitative polymerase chain reaction (RT-qPCR)

156   expressed as the number of viral RNA genomes per mL, and then adjusted to the

157   same concentration (3.8×10^4 copies in 50 μL) for the following experiments. The

158   virus infectivity was determined by a Luc assay expressed as relative

159   luminescence units (RLU). HEK 293T cells expressing human ACE2 (293T-ACE2)

160   were used to test the correlation between ACE2 expression and pseudoviral

161   susceptibility. The vesicular stomatitis virus G (VSV-G) pseudovirus was used as

162   control. As shown in Fig. 3a, both HEK 293T and 293T-ACE2 cells could be

163   effectively transduced by VSV-G pseudovirus. However, the entry of S-D614 and

164   S-G614 pseudoviruses is highly dependent on its cellular receptor ACE2

165   expression. The 293T-ACE2 cells showed an approximately 250-fold and 530-fold

166   increase in Luc activity when transduced by S-D614 and S-G614 pseudoviruses

167   compared to HEK 293T cells, respectively (Fig. 3a). We then detected the

168   inhibitory ability of ACE2-Ig, a fusion protein consisting of the extracellular domain

169   (Met 1-Ser 740) of human ACE2 linked to the Fc region of human IgG1 at the C-

170   terminus[13]. Both S-D614 and S-G614 pseudoviruses were potently inhibited by

171   ACE2-Ig, and the IC_{50} (the concentration causing 50% inhibition of pseudoviral

172   infection) values were 0.13 and 0.15 μg/mL, respectively (Fig. 3b). To further

173   compare the viral entry efficiency meditated by S variants, we detected the Luc

174   activity at different time points post-infection. With the G614 S variant, the increase

8

175 in viral transduction over the D614 variant was 2.2-fold at 48 h post-infection. The

176 highest transduction efficiency (approximately 2.5×10^4 RLU) was observed 72 h

177 post-infection with the S-G614 pseudovirus, which was approximately 2.4-fold

178 higher than that of the S-D614 pseudovirus (Fig. 3c). These data suggest that the

179 D614G mutation in S protein significantly promotes viral entry into ACE2-

180 expressing cells, and ACE2-Ig efficiently blocks both wild-type and mutant S

181 pseudotype virus infection.

182 We next explored the mechanism by which S-G614 increased pseudoviral

183 infectivity. The proteolytic activation of S protein is required for coronavirus

184 infectivity, and the protease-mediated cell-surface pathway is critical for SARS-

185 CoV-2 entry[4]. Since we observed S-G614 could be more efficiently cleaved by the

186 host protease when exogenously expressed in 293T cells, we assumed that host

187 proteases may be involved in the enhancement of S-G614 viral entry. As shown in

188 Fig. 3d, when 293T-ACE2 cells were treated with 100 μg/mL elastase before virus

189 infection, the RLU value in S-G614 pseudovirus-infected cells (6.9×10^4) was

190 about 3.1 fold higher than that of the S-D614 (2.2×10^4), indicating that residue

191 G614 facilitates elastase-induced viral entry. In addition, the clinically proven

192 serine protease inhibitor sivelestat sodium, which is active against elastase, dose-

193 dependently blocked S-G614-driven entry into 293T-ACE2 in the presence of 100

194 μg/mL elastase (Fig. 3e). These data indicated that the infectivity of S-G614

195 pseudovirus containing an additional elastase-2 cleavage site is enhanced by

196 exogenous elastase; therefore, S-G614 pseudovirus is more sensitive to sivelestat

9

197   sodium than the S-D614 pseudovirus.

198   We also tested two other protease inhibitors, camostat mesylate and E-64d, which

199   block host TMPRSS2 and CatB/L, respectively. In 293T-ACE2 cells lacking

200   TMPRSS2, the serine protease inhibitor camostat mesylate did not inhibit S-D614

201   or S-G614 pseudoviral infection (Fig. S1a), while the cysteine protease inhibitor E-

202   64d significantly blocked the entry of these two pseudoviruses, with IC_{50} values of

203   0.37 μM and 0.24 μM for S-D614 and S-G614 pseudoviruses, respectively (Fig.

204   S1b). As expected, these protease inhibitors had no impact on VSV-G pseudovirus

205   infection. Together, these results suggest that S-meditated viral entry into 293T-

206   ACE2 cells deficient in TMPRSS2 is endosomal cysteine protease CatB/L-

207   dependent; therefore, S-D614 and S-G614 pseudoviruses showed similar

208   sensitivity to the CatB/L inhibitor E-64d in 293T-ACE2 cells.

209

210   **Neutralization effect of convalescent sera from patients with COVID-19**

211   **against S-D614 and S-G614 pseudoviruses**

212   Neutralizing antibodies are important for prevention of and possible recovery from

213   viral infections. However, as viruses mutate during replication and spread, host

214   neutralizing antibodies generated in the earlier phase of the infection may not be

215   as effective later on[14,15]. To test whether D614G mutations could affect the

216   neutralization sensitivity of the virus, the neutralization activity of serum samples

217   from convalescent patients with COVID-19 against SARS-CoV-2 S-D614 and S-

218   G614 pseudoviruses were evaluated. To perform the neutralization assay, 50 μL

219   pseudovirus (3.8×10^4 copies) was incubated with serially diluted sera. As shown

220   in Fig. 4a, the inhibition rate of sera from convalescent COVID-19 patients was

221   analyzed at a single dilution of 1:1000, among the 70 tested sera, 65 of them

222   showed neutralizing activities against both S-D614 and S-G614 pseudoviruses

223   with comparable efficiencies. However, five sera samples (patients 1#, 7#, 40#,

224   42# and 52#) showed decreased inhibition rate against the S-G614 pseudovirus.

225   The serum from patient 1# failed to neutralize the S-G614 pseudovirus, even

226   though it neutralized about 30% of the S-D614 pseudovirus at a 1:1000 dilution.

227   Then, the inhibition curves and half-maximal inhibitory dose (ID_{50}) of sera samples

228   from five convalescent patients and one healthy donor were analyzed. Sera from

229   patients 17# and 39#, which were able to neutralize both pseudoviruses to similar

230   degrees, showed similar ID_{50} values (Fig. 4b). However, sera from patients 1#, 7#,

231   40#, 42# and 52# showed relative high neutralizing activity against the S-D614

232   pseudovirus with an ID_{50} ranging from 729 to 1524, but showed decreased

233   neutralizing activity against the S-G614 pseudovirus with an ID_{50} ranging from 216

234   to 367, indicating a 2.5- to 5.9-fold reduction in neutralizing titers (Fig. 4b). These

235   data indicate that most antisera (93%) from patients, likely infected with earlier

236   SARS-CoV-2 variant, can cross neutralize S-G614 variant, although D614G

237   mutation decreases the neutralization sensitivity to 7% convalescent sera.

238

239   **Discussion**

240   Pseudovirus-based assays have been widely used for the study of cellular tropism,

241   receptor recognition, viral inhibitors, and evaluation of neutralizing antibodies

242   without the requirement of BSL-3 laboratories. We constructed pseudotyped

243   SARS-CoV-2 based on the viral S protein using a lentiviral system, which

244   incorporated a Luc reporter gene for easy quantification of coronavirus S protein-

245   mediated entry. We investigated the major mutation in the S protein at position 614

246   and found that serine protease elastase-2 participates in the proteolytic activation

247   of the S-G614 protein, thereby enhancing viral entry into 293T-ACE2 cells (Fig. 5).

248   We demonstrated the potential role of the elastase-2 inhibitor sivelestat in blocking

249   S-G614 pseudovirus infection in the presence of elastase. Although S-D614 and

250   S-G614 variants could be similarly neutralized by most antisera, we found that the

251   S-G614 pseudovirus was more resistant to some neutralizing antisera than S-

252   D614 pseudovirus.

253

254   Several findings stand out in our study: First, we found that the entry efficiency of

255   S-G614 pseudotyped virus was about 2.4 times higher than that of the S-D614

256   pseudovirus when viral input doses were normalized, suggesting that D614G

257   mutation promotes the infectivity of SARS-CoV-2 and enhances viral

258   transmissibility. Since the pseudoviruses were employed in a single round of

259   infection assay, this seemingly small increase in entry activity could cause a large

260   difference in viral infectivity *in vivo*. Yao et al. (2020) reported that a patient-

261   derived viral isolate ZJU-1, which harbors the D614G mutation, has a viral load 19

262   times higher than isolate ZJU-8 (harboring the S-D614) when Vero-E6 cells were

12

263   infected[16]. However, the ZJU-1 isolate contained two other non-synonymous

264   mutations in open reading frame 1a (ORF1a) and envelope (E) gene. Our results

265   also elucidated the cause of increased entry efficiency due to the D614G mutation

266   in the S protein of SARS-CoV-2. The S-G614 protein contains a novel serine

267   protease cleavage site, so it could be cleaved by host elastase-2 more efficiently.

268   Previously studies on SARS-CoV demonstrated that the protease-mediated cell

269   surface entry facilitated a 100- to 1,000-fold increase in efficient infection

270   compared to the endosomal pathway in the absence of proteases[17].

271

272   Second, we found that elastase-enhanced S-G614 pseudoviral infection could be

273   partially blocked by sivelestat sodium. Elastase-2, also known as neutrophil

274   elastase, plays an important role in degenerative and inflammatory diseases.

275   Sivelestat, a drug approved to treat acute respiratory distress syndrome (ARDS) in

276   Japan and South Korea, has a beneficial effect on the pulmonary function of

277   patients with ARDS and systemic inflammatory response syndrome[18]. About 10–

278   15% of patients with COVID-19 progress to ARDS[19]. Since sivelestat may not only

279   mitigate the damage of neutrophil elastase on lung connective tissue, but also limit

280   virus spread by inhibiting S protein processing, Mohamed et al. (2020) advocated

281   the use of sivelestat to alleviate neutrophil-induced damage in critically ill patients

282   with COVID-19[20]. Our *in vitro* results also indicate that sivelestat sodium or similar

283   neutrophil elastase inhibitors might be an effective option for treatment of COVID-

284   19 caused by SARS-CoV-2 harboring the D614G mutation.

13

285

286   Third, we observed that the S-G614 pesudovirus was more resistant to

287 neutralization by convalescent sera from patients, likely infected in mid- to late-

288 January when wild-type (D614) virus was mainly circulating in China. Koyama et

289 al. (2020) reported that D614G is located in one of the predicted B-cell epitopes of

290 SARS-CoV-2 S protein, and this is a highly immunodominant region and may

291 affect the effectiveness of vaccine with wild-type S protein[14]. D614 is conserved in

292 the S protein of SARS-CoV in 2003. Previous studies of SARS-CoV suggested

293 that the peptide $S_{597-625}$ is a major immunodominant peptide in humans and elicits

294 a long-term B-cell memory response after natural infection with SARS-CoV[21].

295 Regions between amino acids 614 and 621 of SARS-CoV-2 S protein were also

296 identified as a B-cell epitope by different methods, and the change in D614G may

297 affect the antigenicity of this region[22]. In our study, we observed that 7% (5/70)

298 convalescent sera showed markedly different neutralization activities between S-

299 G614 and S-G61 protein pseudotyped viruses, indicating that the D614G mutation

300 reduces the sensitivity to neutralizing antibodies from some patients infected with

301 earlier SARS-CoV-2 variant. Whether these patients were at high risk of reinfection

302 with the S-G614 variant should be explored in further studies. It will also be

303 important to determine the breadth of the neutralizing capacity of vaccine-induced

304 neutralizing antibodies.

305

306   Recently, several groups also reported that S-G614 enhances viral infectivity

307   based on pseudovirus assays[23–26], but due to the small sample size, they found no

308   effect on the neutralization sensitivity of the virus[23,24,26]. Given the evolving nature

309   of the SARS-CoV-2 RNA genome, antibody treatment and vaccine design require

310   further considerations to accommodate D614G and other mutations that may

311   affect the immunogenicity of the virus.

312

313   Our study had some limitations. First, 19 amino acids of S protein on the C-

314   terminal were not included in order to improve the packaging efficiency of the

315   SARS-CoV-2 S protein pseudotyped virus, and this pseudovirus only recapitulates

316   viral entry events. Therefore, additional assays with authentic SARS-CoV-2

317   viruses are required. Second, we only tested neutralizing antibodies against the S

318   protein. Previous studies on SARS-CoV indicated that only a small fraction of

319   memory B cells specific for SARS-CoV antigens are directed against neutralizing

320   epitopes present on the S protein[27]. Third, in addition to D614G, further studies on

321   other mutations in the S protein are needed to evaluate their impact on SARS-

322   CoV-2 infectivity, pathogenicity, and immunogenicity. Further studies are needed

323   to determine the impact of these mutations on the severity of COVID-19.

324

325   In summary, we established a SARS-CoV-2 S protein-mediated pseudoviral entry

326   assay and explored the cellular entry of S-D614 and S-G614 pseudotyped viruses.

327   Our study provided evidence that the D614G mutation introduces an additional

328   elastase-2 cut site in the S protein, thereby promoting its cleavage and viral cell

15

329   entry, resulting in SARS-CoV-2 becoming more infectious. Importantly, the D614G

330   mutation reduced the sensitivity of the virus to serum neutralizing antibodies in 7%

331   convalescent patients with COVID-19. Our study will be helpful for understanding

332   SARS-CoV-2 transmission and for the design of vaccines and therapeutic

333   interventions against COVID-19.

334

335   **Materials and Methods**

336   **Plasmids.** The codon-optimized gene encoding SARS-CoV-2 S protein (GenBank:

337   QHD43416) with C-terminal 19-amino acid deletion was synthesized by Sino

338   Biological Inc (Beijing, China), and cloned into the *Kpn*I and *Xba*I restriction sites

339   of pCMV3 vector (pCMV3-SARS-CoV-2-S-C19del, denoted as pS-D614). The

340   D614G mutant S-expressing plasmid (denoted as pS-G614) was constructed by

341   site-directed mutagenesis, with pS-D614 plasmid as a template. The HIV-1 NL4-3

342   ΔEnv Vpr luciferase reporter vector (pNL4-3.Luc.R-E-) constructed by N. Landau[28]

343   was provided by Prof. Cheguo Cai from Wuhan University (Wuhan, China). The

344   VSV-G-expressing plasmid pMD2.G was provided by Prof. Ding Xue from

345   Tsinghua University (Beijing, China). The expression plasmid for human ACE2 was

346   obtained from GeneCopoeia (Guangzhou, China).

347

348   **Cell lines.** HEK 293T cells were purchased from the American Type Culture

349   Collection (ATCC, Manassas, VA, USA). Cells were maintained in Dulbecco's

350   modified Eagle medium (DMEM; Hyclone, Waltham, MA, USA) supplemented with

351 10% fetal bovine serum (FBS; Gibco, Rockville, MD, USA), 100 mg/mL of

352 streptomycin, and 100 units/mL of penicillin at 37 °C in 5% CO_2. HEK 293T cells

353 transfected with human ACE2 (293T-ACE2) were cultured under the same

354 conditions with the addition of G418 (0.5 mg/mL) to the medium. Elastase (from

355 porcine pancreas) was obtained from MACKLIN Biochemical Co. (Shanghai,

356 China).

357

358 **Antibodies and inhibitors.** The anti-RBD monoclonal antibody against the SARS-

359 CoV-2 S protein was kindly provided by Prof. Aishun Jin from Chongqing Medical

360 University. Recombinant human ACE2 linked to the Fc domain of human IgG1

361 (ACE2-Ig) was purchased from Sino Biological Inc. Sivelestat sodium

362 (MedChemExpress, Monmouth Junction, NJ, USA) Camostat mesylate (Tokyo

363 Chemical Industry, Tokyo, Japan), and aloxistatin (E-64d; MedChemExpress) were

364 dissolved in dimethyl sulfoxide (DMSO) at a stock concentration of 50 mM.

365

366 **Sera samples.** A total of 70 convalescent sera samples from patients with COVID-

367 19 (at 2–4 weeks after symptom onset) were collected from three designated

368 hospitals in Chongqing from February 1 to February 10, 2020 (Supplementary

369 information, Table S1). All sera were tested positive using magnetic

370 chemiluminescence enzyme immunoassay (MCLIA) kits supplied by BioScience

371 Co. (Tianjin, China)[29]. Patient sera were incubated at 56 °C for 30 min to inactivate

372 the complement prior to experiments.

373

SARS-CoV-2 genome analysis

The online Nextstrain analysis tool (https://nextstrain.org/ncov) was used to track the D614G mutation in SARS-CoV-2 genomes. All the 2,834 genomes sampled between Dec 20, 2019 and Jun 12, 2020 were visualized using the 'rectangular' layout. The mutations were labeled on branches.

All complete SARS-CoV-2 S gene sequences were downloaded from The National Center for Biotechnology Information (NCBI) website (https://www.ncbi.nlm.nih.gov/sars-cov-2/) on Jun 1, 2020. We obtained 4,701 S coding sequences from NCBI, and after excluding partial and frameshift sequences, 4,649 completed S sequences were used for further analysis. All S nucleotide sequences were translated to amino acid sequences. The nucleotide and amino acid sequences of S were aligned with multiple sequence alignment software MUltiple Sequence Comparison by Log-Expectation (MUSCLE) separately. The 'Wuhan-Hu-1' strain (NC_045512) was used to as the reference sequence, and the mutations were extracted using private PERL scripts.

389

Western blot analysis of SARS-CoV-2 S protein expression. To analyze S protein expression in cells, S-D614- and S-G614-expressing plasmids were transfected into HEK 293T cells. Total protein was extracted from cells using radio immunoprecipitation assay Lysis Buffer (CoWin Biosciences, Beijing, China) containing 1 mM phenylmethylsulfonyl fluoride (Beyotime, Shanghai, China). Equal

18

395   amounts of protein samples were electrophoretically separated by 10% sodium

396   dodecyl sulfate polyacrylamide gel electrophoresis, and then transferred to

397   polyvinylidene difluoride membrane (Millipore, Billerica, MA, USA). The

398   immunoblots were probed with the indicated antibodies. Protein bands were

399   visualized using SuperSignal West Pico Chemiluminescent Substrate kits (Bio-

400   Rad, Hercules, CA, USA) and quantified by densitometry using ImageJ software

401   (NCBI, Bethesda, MD, USA).

402

403   **Production and titration of SARS-CoV-2 S pseudoviruses.** SARS-CoV-2

404   pseudotyped viruses were produced as previously described with some

405   modifications[30]. Briefly, 5×10^6 HEK 293T cells were co-transfected with 6 µg each

406   of pNL4-3.Luc.R-E- and recombinant SARS-CoV-2 S plasmids (pS-D614 or pS-

407   G614) using Lipofectamine 3000 Transfection Reagent (Invitrogen) according to

408   the manufacturer's instructions. The S-D614 and S-G614 protein pseudotyped

409   viruses in supernatants were harvested 48 h after transfection, centrifuged, filtered

410   through a 0.45 µm filter, and stored at −80°C. The pMD2.G was co-transfected

411   with the pNL4-3.Luc.R-E- plasmid to package the VSV-G pseudovirus.

412   The titers of the pseudoviruses were calculated by determining the number of viral

413   RNA genomes per mL of viral stock solution using RT-qPCR with primers and a

414   probe that target LTR[31]. Sense primer: 5′-TGTGTGCCCGTCTGTTGTGT-3′, anti-

415   sense primer: 5′-GAGTCCTGCGTCGAGAGAGC-3′, probe: 5′-FAM-

416   CAGTGGCGCCCGAACAGGGA- BHQ1-3′. Briefly, viral RNAs were extracted

417   using TRIzol (Invitrogen, Rockville, MD) and treated with RNase-free DNase

418   (Promega, Madison, WI, USA) and re-purified using mini columns. Then, the RNA

419   was amplified using the TaqMan One-Step RT-PCR Master Mix Reagents (Applied

420   Biosystems, Thermo Fisher). A known quantity of pNL4-3.Luc.R-E- vector was

421   used to generate standard curves. The S-D614 and S-G614 protein pseudotyped

422   viruses were adjusted to the same titer (copies/mL) for the following experiments.

423

424   **SARS-CoV-2 S-mediated pseudoviral entry assay.** To detect S variant-mediated

425   viral entry, 293T-ACE2 cells (2 × 10^4) grown on 96-well plates were infected with

426   the same amount of S-D614 or S-G614 pseudovirus (3.8 × 10^4 copies in 50 μL).

427   The cells were transferred to fresh DMEM medium 8 h post-infection, and RLU

428   was measured 24-72 h post-infection using Luciferase Assay Reagent (Promega,

429   Madison, WI, USA) according to the manufacturer's protocol[32].

430

431   **Neutralization and inhibition assays.** The 293T-ACE2 cells (2 × 10^4 cells/well)

432   were seeded on 96-well plates. For the neutralization assay, 50 μL pseudoviruses,

433   equivalent to 3.8 × 10^4 vector genomes, were incubated with serial dilutions of

434   sera samples from patients and normal human serum as a negative control for 1 h

435   at 37 °C, then added to the 293T-ACE2 cells (with three replicates for each

436   dilution). For the inhibition assay, the cells were pretreated with elastase for 5 min

437   and then infected with pseudotyped viruses in the presence of various

438   concentrations of sivelestat sodium. After incubation for 12 h, the medium was

20

439 replaced with fresh cell culture medium. Luciferase activity was measured 72 h

440 after infection and the percentage of neutralization was calculated using GraphPad

441 Prism 6.0 software (GraphPad Software, San Diego, CA, USA). Percentage of

442 RLU reduction (inhibition rate) was calculated as: 1- (RLU of sample sera-control

443 wells) / (RLU from mock control sera-control wells)) ×100%. The titers of

444 neutralizing antibodies were calculated as 50% inhibitory dose (ID_{50}).

445

446 **Statistical analyses.** Statistical analyses of the data were performed using

447 GraphPad Prism version 6.0 software. Quantitative data in histograms are shown

448 as means ± SD. Statistical significance was determined using ANOVA for multiple

449 comparisons. Student's *t*-tests were applied to compare the two groups.

450 Differences with *P* values < 0.05 were deemed statistically significant.

451

452 **Ethical approval.** The study was approved by the Ethics Commission of

453 Chongqing Medical University (ref. no. 2020003). Written informed consent was

454 waived by the Ethics Commission of the designated hospital for emerging

455 infectious diseases.

456

457 **Acknowledgments**

469

470   **Author contributions**

471   A-L.H., N.T., and K.W. conceived the project and supervised the study. J.H., C-

472   L.H., Q-Z.G. and G-J.Z. performed most experiments. J.H. and K.W. performed

473   serum neutralization assay. H-J.D. performed SARS-CoV-2 genome analysis. L-Y.

474   H. performed structural analysis of S protein. Q-X.L., J.C. and X-X. C. collected the

475   serum samples. J.H. and Q-Z.G. contributed to the statistical analysis. K.W. and

476   N.T. wrote the manuscript. All the authors analyzed the final data, reviewed and

477   approved the final version.

478

479   **Competing interests**

480   The authors declare no competing interests.

481

482

22

References:

1. Zhou, P. *et al.* A pneumonia outbreak associated with a new coronavirus of probable bat origin. *Nature* **579**, 270–273 (2020).

2. Sanders, J. M., Monogue, M. L., Jodlowski, T. Z. & Cutrell, J. B. Pharmacologic Treatments for Coronavirus Disease 2019 (COVID-19): A Review. *JAMA* (2020) doi:10.1001/jama.2020.6019.

3. Becerra-Flores, M. & Cardozo, T. SARS-CoV-2 viral spike G614 mutation exhibits higher case fatality rate. *Int J Clin Pract* (2020) doi:10.1111/ijcp.13525.

4. Hoffmann, M. *et al.* SARS-CoV-2 Cell Entry Depends on ACE2 and TMPRSS2 and Is Blocked by a Clinically Proven Protease Inhibitor. *Cell* **181**, 271-280.e8 (2020).

5. Du, L. *et al.* The spike protein of SARS-CoV — a target for vaccine and therapeutic development. *Nat Rev Microbiol* **7**, 226–236 (2009).

6. Wrapp, D. *et al.* Cryo-EM structure of the 2019-nCoV spike in the prefusion conformation. *Science* **367**, 1260–1263 (2020).

7. Walls, A. C. *et al.* Structure, Function, and Antigenicity of the SARS-CoV-2 Spike Glycoprotein. *Cell* **181**, 281-292.e6 (2020).

8. Zhou, Y. *et al.* Protease inhibitors targeting coronavirus and filovirus entry. *Antiviral Res* **116**, 76–84 (2015).

9. Bhattacharyya, C. *et al.* Global Spread of SARS-CoV-2 Subtype with Spike Protein Mutation D614G is Shaped by Human Genomic Variations that Regulate Expression of TMPRSS2 and MX1 Genes. *bioRxiv* 2020.05.04.075911 (2020) doi:10.1101/2020.05.04.075911.

505   10. Wrobel, A. *et al.* *Evolution of SARS-CoV-2 spike glycoprotein*.

506   https://www.researchsquare.com/article/rs-29398/v1 (2020) doi:10.21203/rs.3.rs-

507   29398/v1.

508   11. Song, J. *et al.* PROSPER: An Integrated Feature-Based Tool for Predicting Protease

509   Substrate Cleavage Sites. *PLoS ONE* **7**, e50300 (2012).

510   12. Sandrin, V. *et al.* Lentiviral vectors pseudotyped with a modified RD114 envelope

511   glycoprotein show increased stability in sera and augmented transduction of primary

512   lymphocytes and CD34+ cells derived from human and nonhuman primates. *Blood* **100**,

513   823–832 (2002).

514   13. Lei, C. *et al.* Neutralization of SARS-CoV-2 spike pseudotyped virus by recombinant

515   ACE2-Ig. *Nat Commun* **11**, 2070 (2020).

516   14. Koyama, T., Weeraratne, D., Snowdon, J. L. & Parida, L. Emergence of Drift Variants That

517   May Affect COVID-19 Vaccine Development and Antibody Treatment. *Pathogens* **9**, 324

518   (2020).

519   15. Shimizu, Y. K. *et al.* Neutralizing antibodies against hepatitis C virus and the emergence

520   of neutralization escape mutant viruses. *Journal of Virology* **68**, 1494–1500 (1994).

521   16. Yao, H. *et al.* Patient-derived mutations impact pathogenicity of SARS-CoV-2. *medRxiv*

522   2020.04.14.20060160 (2020) doi:10.1101/2020.04.14.20060160.

523   17. Matsuyama, S., Ujike, M., Morikawa, S., Tashiro, M. & Taguchi, F. Protease-mediated

524   enhancement of severe acute respiratory syndrome coronavirus infection. *Proceedings*

525   *of the National Academy of Sciences* **102**, 12543–12547 (2005).

526   18. Okayama, N. *et al.* Clinical effects of a neutrophil elastase inhibitor, sivelestat, in patients

527 with acute respiratory distress syndrome. *J Anesth* **20**, 6–10 (2006).

528 19. Barnes, B. J. *et al.* Targeting potential drivers of COVID-19: Neutrophil extracellular traps.

529 *J Exp Med* **217**, (2020).

530 20. Mohamed, M. M. A. Neutrophil Elastase Inhibitors: A potential prophylactic treatment

531 option for SARS-CoV-2-induced respiratory complications? 2 (2020).

532 21. Wang, Q. *et al.* Immunodominant SARS Coronavirus Epitopes in Humans Elicited both

533 Enhancing and Neutralizing Effects on Infection in Non-human Primates. *ACS Infect Dis*

534 **2**, 361–376 (2016).

535 22. Kim, S.-J., Nguyen, V.-G., Park, Y.-H., Park, B.-K. & Chung, H.-C. A Novel Synonymous

536 Mutation of SARS-CoV-2: Is This Possible to Affect Their Antigenicity and

537 Immunogenicity? *Vaccines* **8**, 220 (2020).

538 23. Zhang, L. *et al.* The D614G mutation in the SARS-CoV-2 spike protein reduces S1

539 shedding and increases infectivity. *bioRxiv* 2020.06.12.148726 (2020)

540 doi:10.1101/2020.06.12.148726.

541 24. Ozono, S. *et al.* Naturally mutated spike proteins of SARS-CoV-2 variants show

542 differential levels of cell entry. *bioRxiv* 2020.06.15.151779 (2020)

543 doi:10.1101/2020.06.15.151779.

544 25. Daniloski, Z., Guo, X. & Sanjana, N. E. The D614G mutation in SARS-CoV-2 Spike

545 increases transduction of multiple human cell types. *bioRxiv* 2020.06.14.151357 (2020)

546 doi:10.1101/2020.06.14.151357.

547 26. Korber, B. *et al.* Tracking changes in SARS-CoV-2 Spike: evidence that D614G increases

548 infectivity of the COVID-19 virus. *Cell* (2020) doi:10.1016/j.cell.2020.06.043.

549   27. Traggiai, E. *et al.* An efficient method to make human monoclonal antibodies from

550   memory B cells: potent neutralization of SARS coronavirus. *Nature Medicine* **10**, 871–

551   875 (2004).

552   28. Connor, R. I., Chen, B. K., Choe, S. & Landau, N. R. Vpr Is Required for Efficient Replication

553   of Human Immunodeficiency Virus Type-1 in Mononuclear Phagocytes. *Virology* **206**,

554   935–944 (1995).

555   29. Long, Q.-X. *et al.* Antibody responses to SARS-CoV-2 in patients with COVID-19. *Nature*

556   *Medicine* 1–4 (2020) doi:10.1038/s41591-020-0897-1.

557   30. Ou, X. *et al.* Characterization of spike glycoprotein of SARS-CoV-2 on virus entry and its

558   immune cross-reactivity with SARS-CoV. *Nature Communications* **11**, 1620 (2020).

559   31. Geraerts, M., Willems, S., Baekelandt, V., Debyser, Z. & Gijsbers, R. Comparison of

560   lentiviral vector titration methods. *BMC Biotechnol* **6**, 34 (2006).

561   32. Shang, J. *et al.* Cell entry mechanisms of SARS-CoV-2. *PNAS* (2020)

562   doi:10.1073/pnas.2003138117.

563

564

26

Table 1. Mutations in spike protein of SARS-CoV-2.

Mutations in Spike Protein	No. of mutation	No. of wildtype	Total No. of sequences	Mutation (%)
D614G	2995	1637	4632	64.659
A829T	37	4602	4639	0.798
L5F	33	4614	4647	0.710
H146Y	26	4594	4620	0.563
P1263L	15	4631	4646	0.323
V483A	12	4387	4399	0.273
S939F	12	4626	4638	0.259
R78M	10	4623	4633	0.216
E583D	9	4639	4648	0.194
A845S	9	4632	4641	0.194

Top 10 abundant non-synonymous mutations observed in S protein of SARS-CoV-2.

27

568   **Figures and Figure legends:**
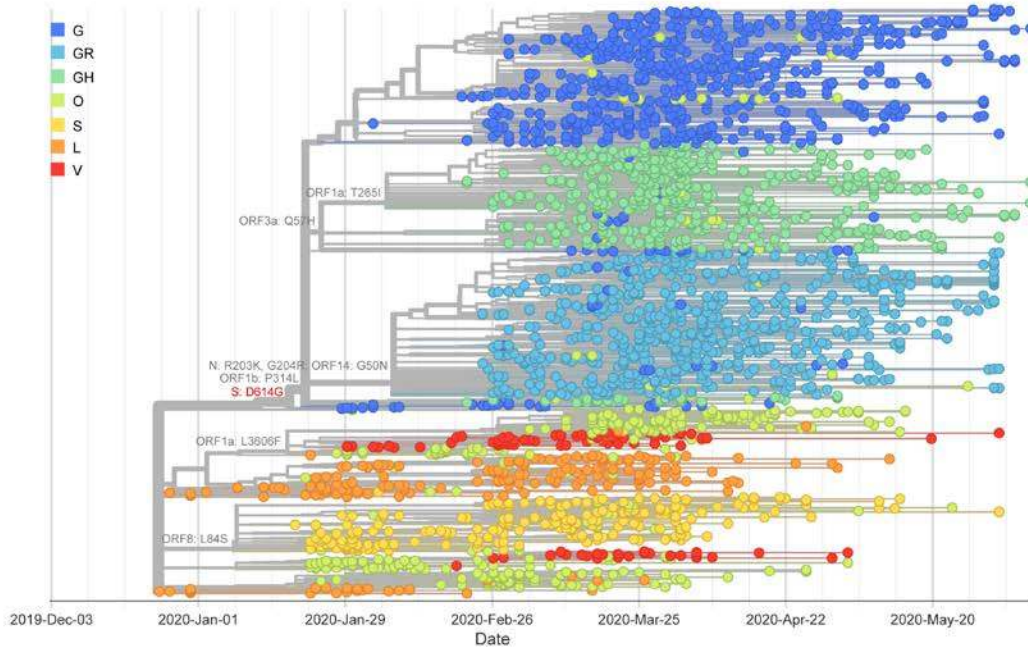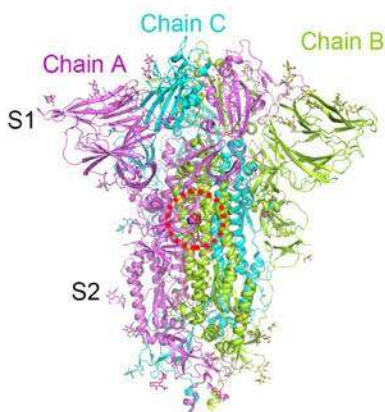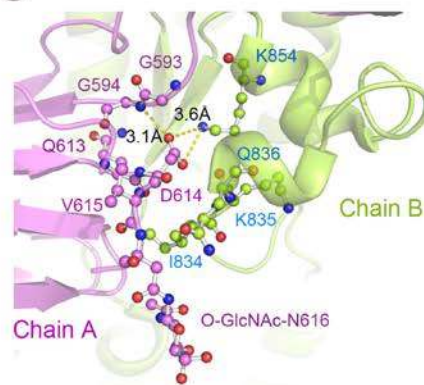
569

570   **Fig. 1. Phylogenetic timetree of SARS-CoV-2 and structural features of its**

571   **spike (S) protein. a** Phylogenetic analysis of SARS-CoV-2 sequences from

28

572   GISAID database. Prevalence of S-D614G genomes over time produced by the

573   Nextstrain analysis tool using GISAID dataset (n = 2,834 genomes samples from

574   January 2020 to May 2020). **b** Cartoon representation of the trimeric SARS-CoV-2

575   spike structure (PBD ID: 6ZGE). Three spike chains are colored in violet, lemon,

576   and aquamarine, respectively. D614 is located at the C-terminal of the S1 subunit

577   and is shown as violet spheres in the red dashed circle. **c** D614 involves the

578   interactions between two S chains. Residues are highlighted by violet or lemon

579   spheres and sticks. Yellow dashed lines indicate hydrogen bonds or salt bridges.

580   PyMOL software (Schrödinger, LLC) was used to generate all rendered structural

581   images.
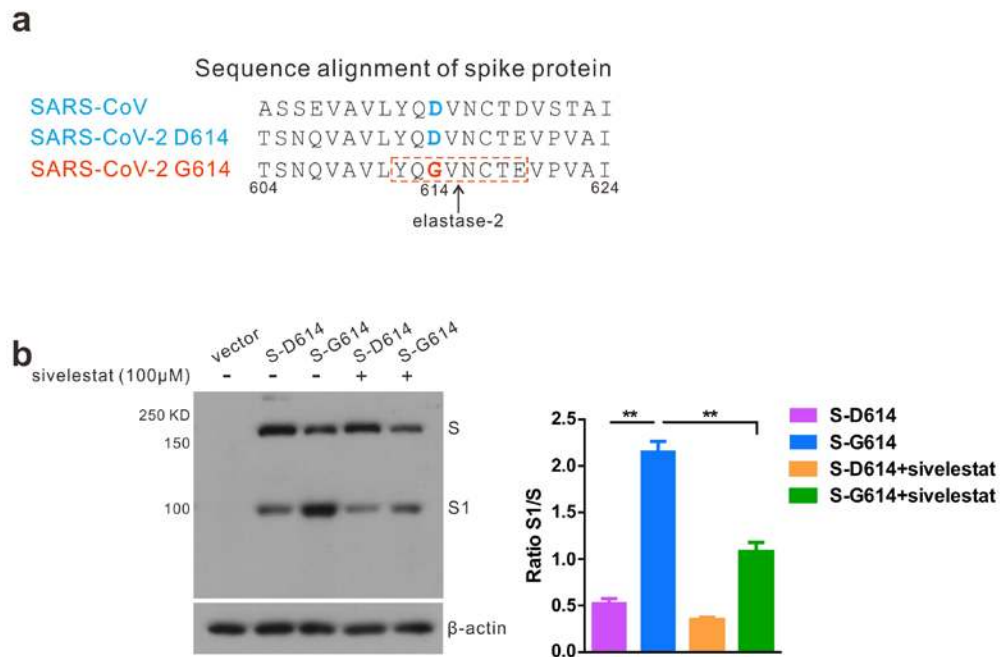
Fig. 2 Detection of S-D614 and S-G614 protein expression and cleavage. a An

additional serine protease (elastase-2) cleavage site in S1-S2 junction was

585 identified in S-614G protein of SARS-CoV-2. **b** Detection of S protein expression

586 in HEK 293T cells by Western blot using the anti-RBD (receptor-binding domain)

587 monoclonal antibody. Cells were transfected with pS-D614 or pS-G614 plasmids

588 or with an empty vector and incubated with or without sivelestat sodium. To

589 compare the S1 and S ratio, integrated density of S1/S was quantitatively

590 analyzed using ImageJ software. n = 3, ±SD. **$P < 0.01$.
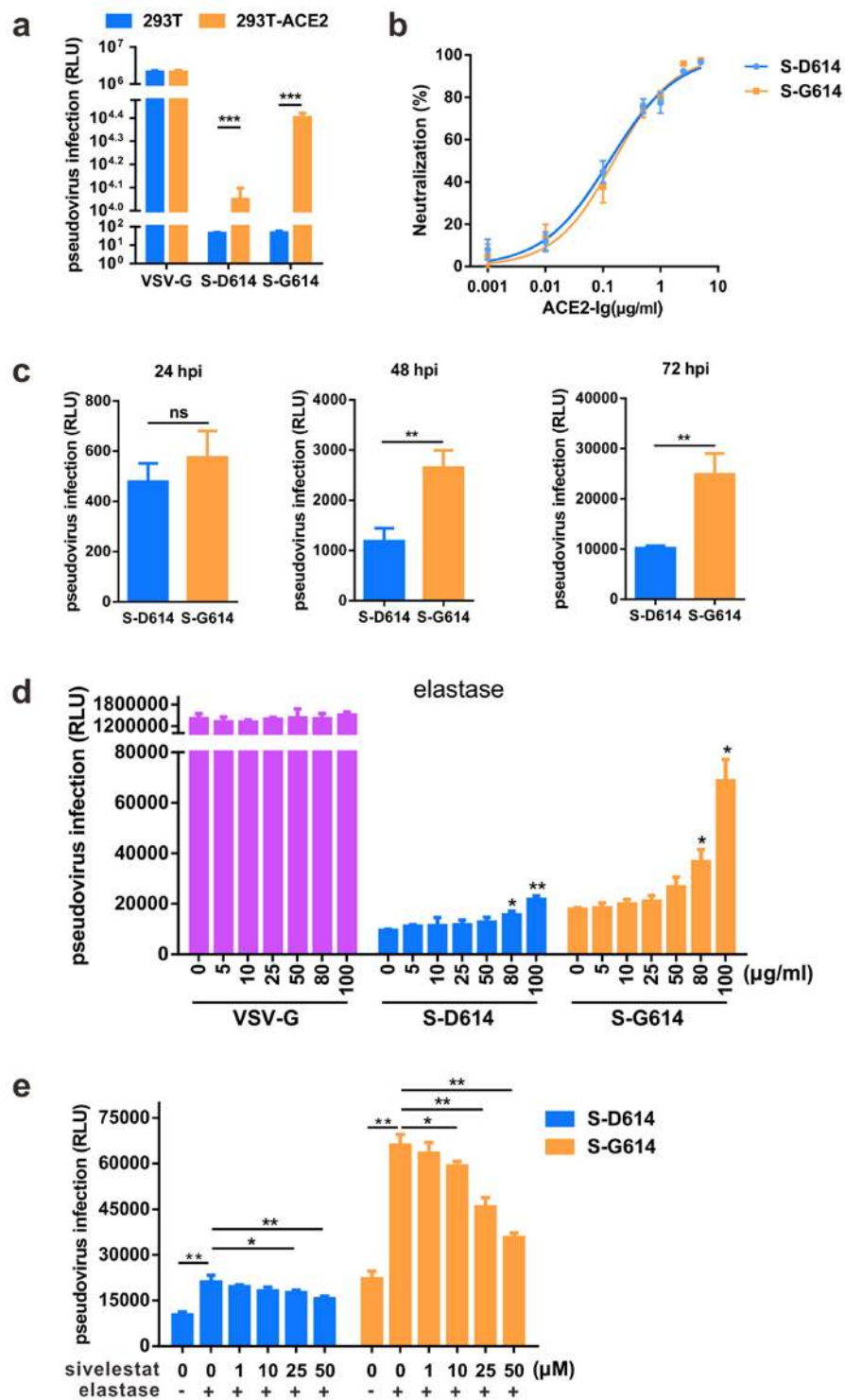
Fig. 3 The S-G614 protein pseudotyped virus showed increased infectivity. a

HEK 293T and 293T-ACE2 (human angiotensin-converting enzyme 2) cells were

594 infected with lentiviruses pseudotyped with VSV-G and SARS-CoV-2 S protein

595 variants. Virus titers were quantified by RT-qPCR and adjusted to 3.8×10^4 copies

596 in 50 μL to normalize input virus doses. The relative luminescence units (RLU)

597 detected 72 h post-infection (hpi). **b** Inhibition of pseudoviral entry by ACE2-Ig.

598 Pseudoviruses were pre-incubated with ACE2-Ig and added to 293T-ACE2 cells,

599 then RLU was measured at 72 hpi. **c** Viral entry efficiency meditated by S variants.

600 The RLU was measured at 24-72 hpi. **d-e** D614G mutation facilitates elastase-2

601 induced pseudoviral entry. 293T-ACE2 cells were treated with elastase for 5 min

602 and then infected with pseudotyped viruses containing the S-D614 or S-G614

603 mutant in the presence of various concentrations of sivelestat sodium. RLU was

604 measured at 72 hpi. n = 3, ±SD. $*P < 0.05$, $**P < 0.01$. ns, not significant.
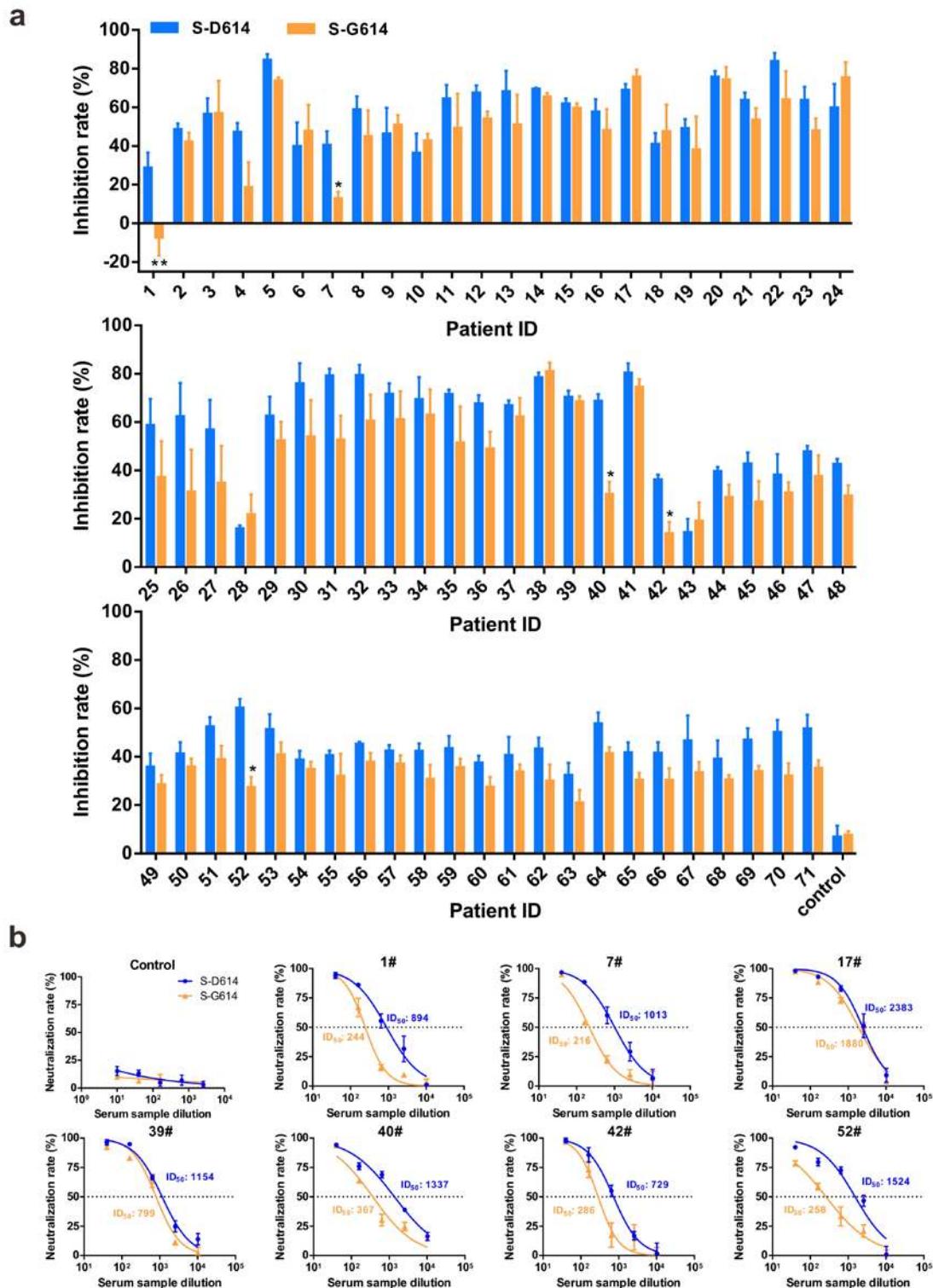
Fig. 4 Detection of neutralizing antibodies in convalescent sera against spike (S)-D614 and S-G614 protein pseudotyped viruses. a The inhibition rate of

608   convalescent sera from 70 patients with COVID-19 against S-D614 and S-G614

609   pseudoviruses. A serum sample from healthy individual was tested as a negative

610   control. Convalescent sera were collected 2–4 weeks after symptom onset from

611   confirmed case patients (1#–70#). Sera was analyzed at a single dilution of

612   1:1000. RLU was measured at 72 hpi. We then compared the RLU of serum

613   neutralized sample to the control and calculated the inhibition rate. n = 3, ±SD. **b**

614   The inhibition curves for serum samples from seven convalescent patients and a

615   healthy donor. The initial dilution was 1:40, followed by 4-fold serial dilution.

616   Neutralization titers were calculated as 50% inhibitory dose (ID_{50}), expressed as

617   the serum dilution at which RLUs were reduced by 50% compared with virus

618   control wells after subtraction of background RLU in cell control wells.

619
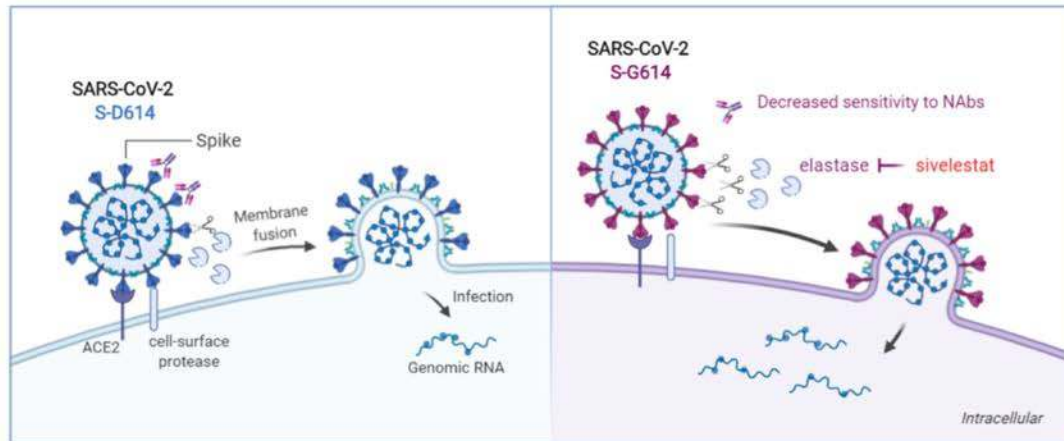
Fig. 5 Proposed working model of this study. Protease-mediated cell-surface

pathway is critical for SARS-CoV-2 entry and infection. D614G mutation introduces

623   an additional elastase-2 cut site in the spike protein of SARS-CoV-2, thereby

624   promoting its cleavage and enhancing viral entry into host cells. The elastase-2

625   inhibitor sivelestat partially blocks S-G614 pseudovirus infection in the presence of

626   elastase. Both S-D614 and S-G614 variants could be similarly neutralized by most

627   antisera, however, S-G614 mutant is more resistant to neutralizing antibodies

628   (NAbs) from some patients infected with earlier SARS-CoV-2 variant.